[논 문] 한국재료학회지
Kor. J. Mater. Res.
Vol. 23, No. 5 (2013)
http://dx.doi.org/10.3740/MRSK.2013.23.5.266

Hydrogen Storage Properties of Pure MgH_2

Young Jun Kwak, Seong Ho Lee, Hye Ryoung Park* and Myoung Youp Song**†

Department of Materials Engineering, Graduate School, Chonbuk National University, 567 Baekje-daero Deokjin-gu, Jeonju 561-756, Korea
*Faculty of Applied Chemical Engineering, Chonnam National University, 77 Yongbong-ro Buk-gu, Gwangju 500-757, Korea
**Division of Advanced Materials Engineering, Department of Hydrogen and Fuel Cells, Hydrogen & Fuel Cell Research Center, Engineering Research Institute, Chonbuk National University, 567 Baekje-daero Deokjin-gu, Jeonju 561-756, Korea

(Received March 11, 2013 : Received in revised form April 17, 2013 : Accepted April 18, 2013)

Abstract The hydrogen storage properties of pure MgH_2 were studied and compared with those of pure Mg. At the first cycle, pure MgH_2 absorbed hydrogen very slowly at 573 K under 12 bar H_2. The activation of pure MgH_2 was completed after three hydriding-dehydriding cycles. At the 4th cycle, the pure MgH_2 absorbed 1.55 wt% H for 5 min, 2.04 wt% H for 10 min, and 3.59 wt% H for 60 min, showing that the activated MgH_2 had a much higher initial hydriding rate and much larger H_a (60 min), quantity of hydrogen absorbed for 60 min, than did activated pure Mg. The activated pure Mg, whose activation was completed after four hydriding-dehydriding cycles, absorbed 0.80 wt% H for 5 min, 1.25 wt% H for 10 min, and 2.34 wt% H for 60 min. The particle sizes of the MgH_2 were much smaller than those of the pure Mg before and after hydriding-dehydriding cycling. The pure Mg had larger hydrogen quantities absorbed at 573K under 12 bar H_2 for 60 min, H_a (60 min), than did the pure MgH_2 from the number of cycles $n = 1$ to $n = 3$; however, the pure MgH_2 had larger H_a (60 min) than did the pure Mg from $n = 4$ to $n = 6$.

Key words pure magnesium hydride, pure magnesium, hydriding rate, microstructure, X-ray diffraction.

1. Introduction

Magnesium has advantages as a hydrogen storage material from the viewpoints of hydrogen storage capacity, cost and reserves in the earth's crust. However, its reaction rate with H_2 is very low.[1)]

Song's review[2)] on the kinetic studies of the hydriding and the dehydriding reactions of Mg reported that the hydriding and dehydriding reactions of Mg are nucleation-controlled under certain conditions and progress by a mechanism of nucleation and growth, and that the hydriding rates of Mg are controlled by the diffusion of hydrogen through a growing Mg hydride layer.

By use of the first-principles density functional theory for a cluster model, the alloying effect of transition element M on the electronic structure of magnesium hydride, MgH_2, was investigated by Chen et al.[3)]. They concluded that the chemical interaction between Mg and H may play a dominant role in the pure MgH_2 system. Such a strong interaction remained in the alloyed $Mg(M)H_2$ when the central Mg was replaced by an alloying element M. By a satisfactory fit of the calculated M (or Mg)-H interactions with the enthalpies of formation for some pure dihydrides, they reported that 70 % chemical (ionic plus covalent) interactions would appear to be ionic but the covalent interaction of an adjacent Mg to M with a H atom around it would be sensitive to the substitution of M.

The paper of Matović et al.[4)] dealt with non-isothermal kinetics models of hydrogen desorption from MgH_2 altered by ion bombardment and stressed the importance of the MgH_2 surface during its decomposition. In the case of argon-irradiated samples, where defects were induced in the near-surface region, the Avrami Erofeev mechanism with parameter $n = 2$ could be adopted while in the case of

†Corresponding author
E-Mail : songmy@jbnu.ac.kr (M. Y. Song, Chonbuk Nat'l Univ.)

boron-irradiated samples, where defects were created deeper in the bulk, the desorption mechanism was the same with n = 3. The difference was possibly related to the concentration and good dispersion of defects in near-surface region in the samples.

A lot of work to improve the hydriding and dehydriding rates of magnesium has been performed by alloying with magnesium metals[5,6] such as Cu,[7] Ni,[8,9] In,[10] Sn,[11] V,[12] and Ni and Y,[13] by synthesizing compounds such as $CeMg_{12}$[14] and $Mg_{76}Ti_{12}Fe_{12-x}Ni_x$ (x = 4, 8),[15] and by making composites such as Mg- 20 wt% $Fe_{23}Y_8$.[16] Aminorroaya et al.[17] added Nb and multi-walled carbon nanotubes to Mg-Ni alloys, and Cho et al.[18] added transition metals to cast Mg-Ni alloys for the improvement of the reaction rates of Mg with H_2. Milanese et al.[19] mixed Ni and Cu with Mg, Tanguy et al.[20] mixed metal additives with magnesium, and Eisenberg et al.[21] plated nickel on the surface of magnesium to improve the hydriding-dehydriding kinetics of MgH_2.

Mao et al.[22] investigated doping MgH_2 with $NiCl_2$ and $CoCl_2$ in an effort to develop MgH_2 with a low dehydriding temperature and fast sorption kinetics. Both the dehydrogenation temperature and the absorption/desorption kinetics were improved by adding either $NiCl_2$ or $CoCl_2$, and a significant enhancement was obtained in the case of the $NiCl_2$ doped sample.

The paper of Cermak and David [23] investigated separate catalytic effects of Ni, Mg_2Ni and Mg_2NiH_4 on the hydrogen desorption characteristics of MgH_2. It was observed that the catalytic efficiency of Mg_2NiH_4 was considerably higher than that of pure Ni and non-hydrated intermetallic Mg_2Ni.

As shown in these examples, the hydrogen absorption and desorption behaviors of Mg have been studied by using pure Mg or pure MgH_2 as a starting material. The pure MgH_2 is more difficult to synthesize and more expensive than the pure Mg. By comparing the hydrogen absorption and desorption behaviors and the prices, it is necessary to determine which is appropriate to be used as a starting material.

In this work, hydrogen storage properties of the pure MgH_2 were studied and compared with those of the pure Mg.

2. Experimental details

Pure MgH_2 powder (hydrogen storage grade, Aldrich) and pure Mg powder (−100 + 200 mesh, 99.6 %, Alfa Aesar) were used.

The absorbed or desorbed hydrogen quantity was measured as a function of time by a volumetric method, using a Sivert's type hydriding and dehydriding apparatus described previously.[24] 0.5 g of the samples was used for these measurements. Samples after reactive mechanical grinding and those after hydriding-dehydriding cycling were characterized by X-ray diffraction (XRD) with Cu Kα radiation, using a Rigaku D/MAX 2500 powder diffractometer. The microstructures of the powders were observed by a JSM-6400 scanning electron microscope (SEM) operated at 20 kV.

3. Results and discussion

The percentage of absorbed hydrogen, H_a, is expressed with respect to sample weight. Fig. 1 shows the variation of the H_a versus t curve with the number of cycles, n, for the pure Mg at 573 K under 12 bar H_2. The pure Mg absorbs hydrogen very slowly. At n = 1, pure Mg absorbs 0.05 wt% H for 5 min, 0.08 wt% H for 10 min, 0.17 wt% H for 30 min, and 0.29 wt% H for 60 min. The quantity of hydrogen absorbed for 60 min is expressed by H_a (60 min). The initial hydriding rate and H_a (60 min) increase as the number of cycles increases from n = 1 to n = 5, and then decrease as the number of cycles increases from n = 5 to n = 6, showing that the activation of the pure Mg was completed after four hydriding-dehydriding cycles. At n = 5, pure Mg absorbs 0.80 wt% H for 5 min, 1.25 wt% H for 10 min, 1.94 wt% H for 30 min, and 2.34 wt% H for 60 min.

Dehydriding rate at 573 K under 1.0 bar H_2 was too low to be measured, and thus the sample was dehydrided at 623 K in vacuum for 2 h for the hydrogen absorption measurement at the next cycle.

The SEM micrographs of the pure Mg and the pure Mg dehydrided at the 10th hydriding-dehydriding cycle are shown in Fig. 2. The particle of the pure Mg has a few cracks with quite flat surface. In the pure Mg dehydrided at the 10th hydriding-dehydriding cycle, defects

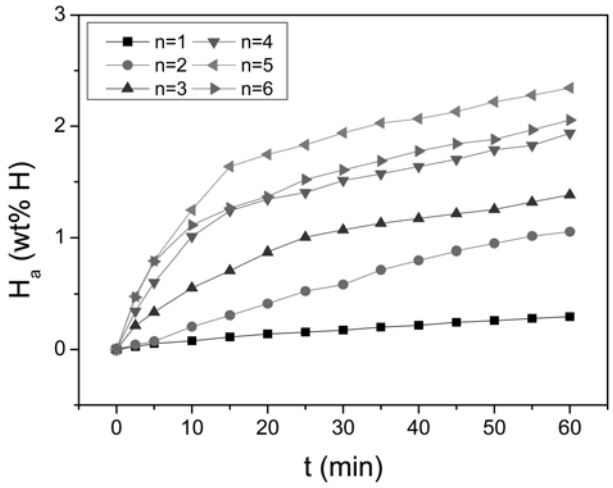

Fig. 1. Variation of the H_a versus t curve with the number of cycles, n, for pure Mg at 573 K under 12 bar H_2.

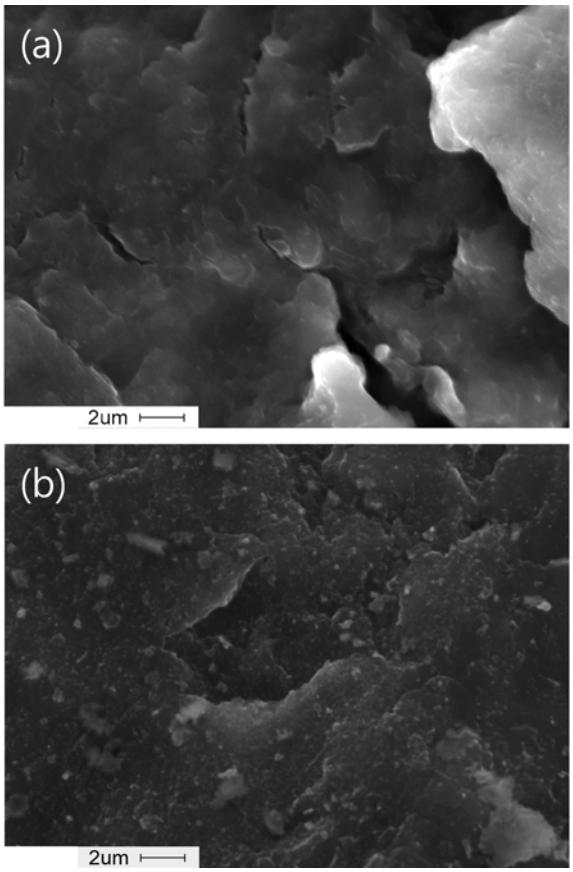

Fig. 2. SEM micrographs of (a) the pure Mg, and (b) the pure Mg dehydrided at the 10th hydriding-dehydriding cycle.

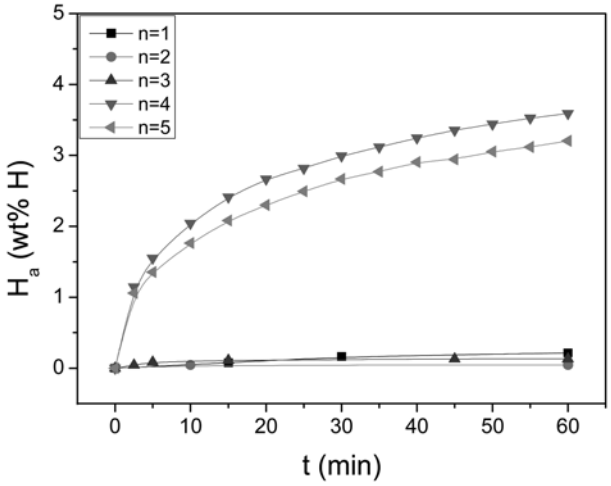

Fig. 3. Variation of the H_a versus t curve with the number of cycles for the pure MgH_2 at 573 K under 12 bar H_2.

are created with hydriding-dehydriding cycling. The expansion and contraction of Mg with the hydriding and dehydriding reactions is considered to create defects.

Fig. 3 shows the variation of the H_a versus t curve with the number of cycles, n, for the pure MgH_2 at 573 K under 12 bar H_2. At n = 1, the sample absorbs hydrogen very slowly. The initial hydriding rate and H_a (60 min) of the MgH_2 increase as the number of cycles increases from n = 1 to n = 4, and decrease as the number of cycles increases from n = 4 to n = 5, showing that the activation of the pure MgH_2 was completed after three hydriding-dehydriding cycles. At n = 4, the MgH_2 absorbs 1.55 wt% H for 5 min, 2.04 wt% H for 10 min, 2.99 wt% H for 30 min, and 3.59 wt% H for 60 min, showing that the MgH_2 has a much higher hydriding rate than the activated pure Mg. The increase in the initial hydriding rate and H_a (60 min) with cycling from n = 1 to n = 3 are low, but they are high from n = 4 to n = 6. The particle expands during hydriding and contracts during dehydriding. For the first two hydriding-dehydriding cycles, the formation of cracks and the deminution of particle size due to expansion and contraction of particles may occur weakly, but they occur probably strongly at the 3rd hydriding-dehydriding cycle, leading to the high hydriding rate.

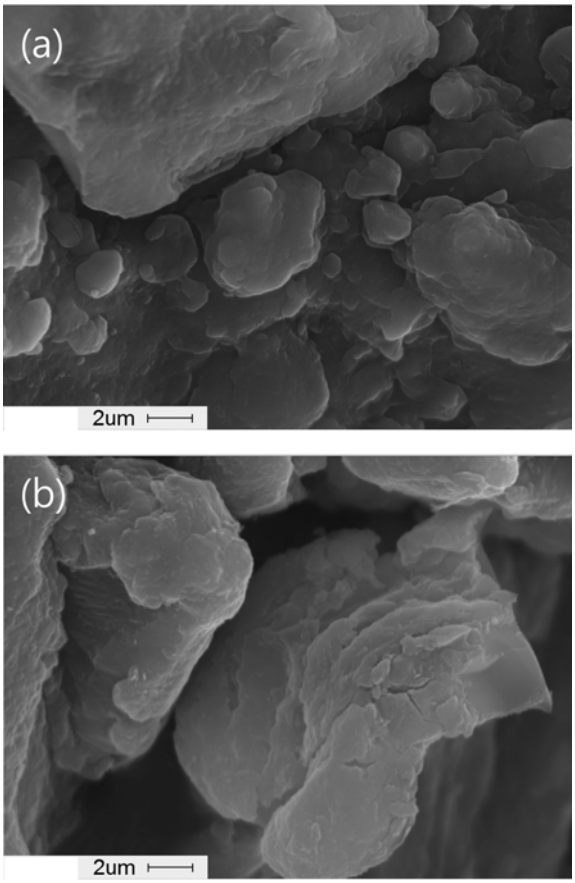

Fig. 4. SEM micrographs of (a) the pure MgH_2, and (b) the pure MgH_2 dehydrided at the 7th hydriding-dehydriding cycle.

The SEM micrographs of the pure MgH_2 and the pure MgH_2 dehydrided at the 7th hydriding-dehydriding cycle are shown in Fig. 4. The pure MgH_2 has small and large particles with quite flat surfaces. The particle size of the

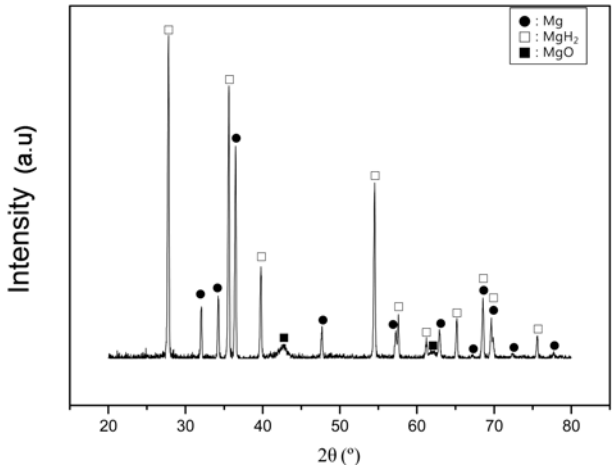

Fig. 5. XRD pattern of the pure MgH_2 dehydrided at the 7th hydriding-dehydriding cycle.

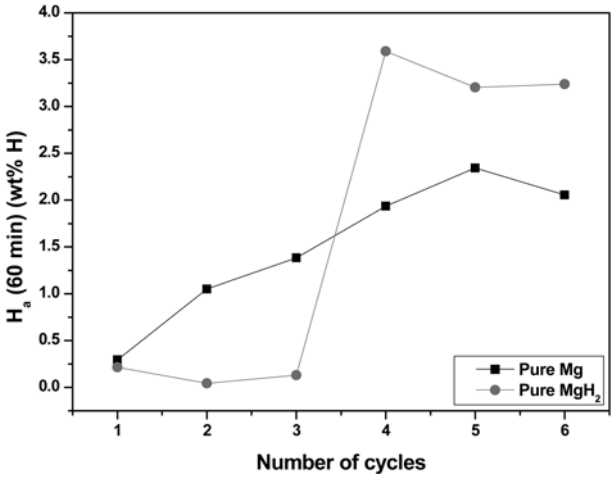

Fig. 6. Variations of hydrogen quantity absorbed at 573 K under 12 bar H_2 for 60 min, Ha (60 min), with the number of cycles from 1 to 6 for the pure Mg and the pure MgH_2.

pure MgH_2 is much smaller than that of the pure Mg. In the pure MgH_2 dehydrided at the 7th hydriding-dehydriding cycle, defects are created with hydriding-dehydriding cycling. The expansion and contraction of Mg with the hydriding and dehydriding reactions is considered to make defects. The particle size of the pure MgH_2 after hydriding-dehydriding cycling is similar to that of the pure MgH_2 before hydriding-dehydriding cycling. The particle size of the pure MgH_2 after hydriding-dehydriding cycling is smaller than that of the pure Mg after hydriding-dehydriding cycling. This is resulted partly from the point that the initial particle size (before hydriding-dehydriding cycling) of MgH_2 was smaller than that of the pure Mg.

Fig. 5 shows the XRD pattern of the pure MgH_2 dehydrided at the 7th hydriding-dehydriding cycle. The sample contains Mg, a small amount of MgO and a large amount of MgH_2, indicating that a large fraction of MgH_2 remains even after dehydriding in vacuum at 623 K for 2 h, and showing that the dehydriding rate of the pure MgH_2 is very low.

Variations of the hydrogen quantity absorbed at 573 K under 12 bar H_2 for 60 min, H_a (60 min), with the number of cycles from 1 to 6 for the pure Mg and the pure MgH_2 are shown in Fig. 6. The value of H_a (60 min) for the pure Mg increases as the number of cycles increases from n = 1 to n = 5, and decreases from n = 5 to n = 6. The values of H_a (60 min) for the pure Mg are 0.29, 2.34, and 2.06 wt% H at n = 1, 5, and 6, respectively. The value of H_a (60 min) for the pure MgH_2 increases as the number of cycles increases from n = 1 to n = 4, and decreases from n = 4 to n = 6. The values of H_a (60 min) for the pure MgH_2 are 0.22, 3.59, and 3.24 wt% H at n = 1, 4, and 6, respectively. The pure Mg has larger values of H_a (60 min) than the pure MgH_2 from n = 1 to n = 3, but the pure MgH_2 has larger values of H_a (60 min) than the pure Mg from n = 4 to n = 6.

The pure MgH_2 dehydrided at the 7th hydriding-dehydriding cycle contains Mg, a small amount of MgO and a large amount of MgH_2 (Fig. 5). Since MgH_2 remains before hydriding measurement, the nuclei of MgH_2 are present before hydriding measurement. Before hydridig measurement, more MgH_2 remained in the pure MgH_2 than in the pure Mg. Fig. 2(b) and Fig. 4(b) show that the particle size of the pure MgH_2 after hydriding-dehydriding cycling is smaller than that of the pure Mg after hydriding-dehydriding cycling. The larger content of MgH_2 (thus the larger content of MgH_2 nuclei) and the smaller particle size of the pure MgH_2 are believed to lead to the higher initial hydriding rate and larger H_a (60 min) of the pure MgH_2 than the pure Mg.

4. Conclusions

At the first cycle, the pure MgH_2 absorbed hydrogen very slowly at 573 K under 12 bar H_2. The activation of the pure MgH_2 was completed after three hydriding-dehydriding cycles. At the 4th cycle, the pure MgH_2 absorbed 1.55 wt% H for 5 min, 2.04 wt% H for 10 min, and 3.59 wt% H for 60 min, showing that the activated MgH_2 had a much higher initial hydriding rate and a much larger H_a (60 min) than the activated pure Mg. The activated pure Mg, whose activation was completed after four hydriding-dehydriding cycles, absorbed 0.80 wt% H for 5 min, 1.25 wt% H for 10 min, and 2.34 wt% H for 60 min. The particle sizes of the pure MgH_2 before and after hydriding-dehydriding cycling were much smaller than those of the pure Mg before and after hydriding-dehydriding cycling. The pure Mg had larger values of H_a (60 min) than the pure MgH_2 from the number of cycles n = 1 to n = 3, but the pure MgH_2 had larger values of H_a

(60 min) than the pure Mg from n = 4 to n = 6.

Acknowledgement

This research was supported by Basic Science Research Program through the National Research Foundation (NRF) of Korea funded by the Ministry of Education, Science and Technology (Grant number 2011-0023566).

This work was also supported by the selection of research oriented professor of Chonbuk National University in 2013.

References

1. M. Y. Song, Y. J. Kwak, B. S. Lee, H. R. Park and B. G. Kim, Korean J. Met. Mater., **49**(12), 989 (2011).
2. M. Y. Song, J. Mater. Sci., **30**, 1343 (1995).
3. D. Chen, Y. M. Wang, L. Chen, S. Liu, C. X. Ma, L. B. Wang, Acta Materialia, **52**(2), 521 (2004).
4. L. Matović, S. Kurko, Ž. Rašković-Lovre, R. Vujasin, I. Milanović, S. Milošević, J. Grbović Novaković, Int. J. Hydrogen Energy, **37**(8), 6727 (2012).
5. S. H. Hong, S. N. Kwon, and M. Y. Song, Korean J. Met. Mater., **49**(4), 298 (2011).
6. K. I. Kim and T. W. Hong, Korean J. Met. Mater., **49**(3), 264 (2011).
7. J. J. Reilly and R. H. Wiswall, Inorg. Chem., **6**(12), 2220 (1967).
8. J. J. Reilly and R. H. Wiswall Jr, Inorg. Chem., **7**(11), 2254 (1968).
9. E. Akiba, K. Nomura, S. Ono and S. Suda, Int. J. Hydrogen Energy, **7**(10), 787 (1982).
10. M. H. Mintz, Z. Gavra and Z. Hadari, J. Inorg. Nucl. Chem., **40**, 765 (1978).
11. H. C. Zhong, H. Wang, L. Z. Ouyang, M. Zhu, J. Alloy Compd., **509**(11), 4268 (2011).
12. P. Pei, X. Song, J. Liu, A. Song, P. Zhang, G. Chen, Int. J. Hydrogen Energy, **37**(1), 984 (2012).
13. Z. Li, X. Liu, L. Jiang, S. Wang, Int. J. Hydrogen Energy, **32**(12), 1869 (2007).
14. J. M. Boulet and N. Gerard, J. Less-Common Met., **89**, 151 (1983).
15. M. Lucaci, Al. R. Biris, R. L. Orban, G. B. Sbarcea, V. Tsakiris, J. Alloys Compd., **488**(1), 163 (2009).
16. Z. Li, X. Liu, Z. Huang, L. Jiang, S. Wang, Rare Metals, **25**(6)(Supplement 1), (247) 2006.
17. S. Aminorroaya, A. Ranjbar, Y. H. Cho, H. K. Liu, A. K. Dahle, Int. J. Hydrogen Energy, **36**(1), 571 (2011).
18. Y. H. Cho, S. Aminorroaya, H. K. Liu, A. K. Dahle, Int. J. Hydrogen Energy, **36**(8), 4984 (2011).
19. C. Milanese, A. Girella, G. Bruni, P. Cofrancesco, V. Berbenni, P. Matteazzi, A. Marini, Intermetallics, **18**(2), 203 (2010).
20. B. Tanguy, J. L. Soubeyroux, M. Pezat, J. Portier and P. Hagenmuller, Mater. Res. Bull., **11**, 1441(1976).
21. F. G. Eisenberg, D. A. Zagnoli and J. J. Sheridan III, J. Less-Common Met., **74**, 323 (1980).
22. J. Mao, Z. Guo, X. Yu, H. Liu, Z. Wu, J. Ni, Int. J. Hydrogen Energy, **35**(10), 4569 (2010).
23. J. Cermak, B. David, Int. J. Hydrogen Energy, **36**(21), 13614 (2011).
24. M. Y. Song, S. H. Baek, J. -L. Bobet, and S. H. Hong, Int. J. Hydrogen Energy, **35**, 10366 (2010).